Collective excitations in truncated semiconductor superlattices in a transverse magnetic field

Manvir S. Kushwaha
Departamento de Física del Instituto de Ciencias, Universidad Autónoma de Puebla, Apartado Postal J-48, Puebla 72570, Mexico
(Received 22 April 1988; revised manuscript received 1 March 1989)

We consider the propagation of bulk and surface magnetoplasmons in a semi-infinite superlattice structure composed of alternating materials A and B. Implicit general dispersion relations for bulk and surface magnetoplasmons are derived allowing the dielectric tensor ($\tilde{\epsilon}$) of each material to be a function of frequency and magnetic field ($\mathbf{B}_0$). The external magnetic field is taken to be parallel to the superlattice axis (or perpendicular to the interfaces). The nonradiative magnetoplasma modes (polaritons) are characterized by the electromagnetic fields which decay exponentially away from the interfaces. We present numerical results for a number of illustrative cases including the effect of retardation.

I. INTRODUCTION

With the recent advancement of molecular-beam epitaxy, early predictions by Esaki,[1] of the possibility to artificially construct metallic or semiconductor superlattices with high precision, are now possible. This has stimulated a considerable theoretical and experimental research interest to study the electronic and optical properties of particular semiconductor superlattices. Studies of collective excitations are fundamental to a complete understanding of these tailor-made materials. The set of such excitations is characterized by a wave vector ($q_\perp$) normal to the interfaces as well as a wave vector ($q_\parallel$) parallel to the interfaces. If d is the width of the unit cell of the superlattice, the boundaries of the bulk plasmon bands exist for $q_\perp = 0$ or π. The truncation of the superlattice yields surface plasmon-polariton modes located at the surface but still affected by the layered structure of the bulk constituents. These polariton modes occur in the gaps between the bulk bands, and above and below the bands.

The effect of an applied magnetic field on carrier transport at semiconductor interfaces has long been of great interest. The application of an external magnetic field in thin-films and multilayered heterostructures has been shown to cause interesting qualitative changes in the behavior characteristic of the interface excitations.[2–4] This is because the magnetic field quantizes the component of the electron energy associated with its transverse motion. In the presence of an applied magnetic field ($\mathbf{B}_0$), there are three main configurations[2] out of which the case where $\mathbf{B}_0$ is perpendicular to the interfaces (as is the case here) and parallel to the confining electric field is a very special one. This is because only then does the system attain the state of complete quantization, and this provides an ideal tool for studying the quantum transport phenomena.[5]

In the recent past, the elementary excitations in superlattice systems have been studied by a number of authors using macroscopic as well as microscopic theories,[6–15] with and without an applied magnetic field. There are usually two situations. (i) The case where the layer widths are much smaller than the electron mean free path and the electrons are quantized into a series of miniband energy levels (usually referred to as the *quantum limit*). In this case the conduction electrons correspond to those of a quasi-two-dimensional electron gas and their dynamical behavior cannot be described by the usual dielectric function of a three-dimensional electron gas. (ii) The case where the layer widths are much larger than the electron mean free path so that the quantum-mechanical effects are negligible and the layers can be treated as bulk constituents whose properties can be described by macroscopic dielectric functions (usually referred to as the *classical limit*).

In this paper our aim is to study the collective (bulk and surface) excitations of a semiconductor superlattice subjected to an external magnetic field oriented perpendicular to the interfaces in the classical limit. We use Maxwell's equations and standard electromagnetic boundary conditions to obtain the dispersion relations of the superlattice magnetoplasmons. Since the resultant (superlattice) structure is periodic, its elementary excitations have properties which are determined essentially by imposing Bloch's theorem.

The rest of the paper is organized as follows. In Sec. II we describe the model and obtain the dispersion relation for bulk magnetoplasmons of an infinite superlattice and then that for surface magnetoplasma polaritons of a truncated superlattice. In Sec. III we present the dispersion curves for the superlattice found by numerically solving the dispersion relations derived in Sec. II for specific material parameters. Finally, Sec. IV contains our conclusions.

II. THEORY

We consider the superlattice structure depicted in Fig. 1. Material A has a frequency- and magnetic-field-dependent dielectric tensor $\tilde{\epsilon}_A$ and thickness d_A, while

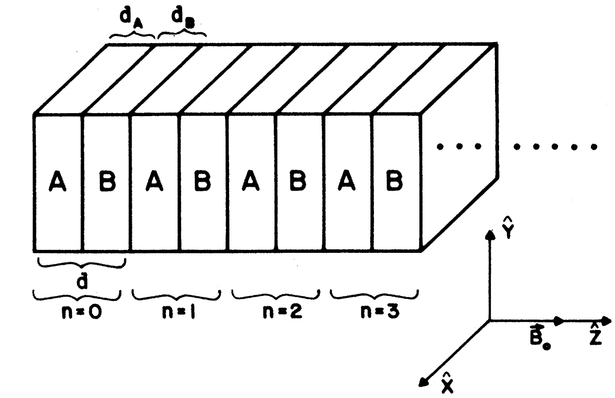

FIG. 1. Schematics of a periodic semiconductor heterostructure consisting of two different types of dielectric slabs.

the material B has dielectric tensor $\tilde{\epsilon}_B$ and thickness d_B. The unit cell of the structure has a width $d = d_A + d_B$. The magnetoplasmons are assumed to propagate along the y direction parallel to the interfaces with wave vector q_y and frequency ω. The external magnetic field is imposed in the z direction; it is therefore perpendicular to both the direction of propagation and the interfaces. We will study the collective magnetoplasma excitations characterized by the electromagnetic fields decaying exponentially away from the interfaces.

A. Infinite superlattice

Elimination of magnetic field vector (**B**) from Maxwell's curl field equations yields the following wave equation in terms of the macroscopic electric field (**E**):

$$\nabla \times (\nabla \times \mathbf{E}) - q_0^2 \tilde{\epsilon} \cdot \mathbf{E} = \mathbf{0} , \tag{1}$$

where $q_0 = \omega / c$ is the vacuum wave vector. We assume the spatial and temporal dependence of the fields to have the form $\sim e^{i(\mathbf{q}\cdot\mathbf{r} - \omega t)}$. In the absence of an applied magnetic field ($\mathbf{B}_0$) each bulk constituent is assumed to be isotropic. In the presence of $\mathbf{B}_0$, the wave-field equation can be rewritten as follows:

$$\begin{bmatrix} \epsilon_{xx} q_0^2 - q_y^2 - q_z^2 & \epsilon_{xy} q_0^2 & 0 \\ -\epsilon_{xy} q_o^2 & \epsilon_{xx} q_0^2 - q_z^2 & q_y q_z \\ 0 & q_y q_z & \epsilon_{zz} q_0^2 - q_y^2 \end{bmatrix} \begin{bmatrix} E_x \\ E_y \\ E_z \end{bmatrix} = \begin{bmatrix} 0 \\ 0 \\ 0 \end{bmatrix} , \tag{2}$$

where $\epsilon_{xx} = \epsilon_L [1 - \omega_p^2 / (\omega^2 - \omega_c^2)]$, $\epsilon_{xy} = i \epsilon_L \omega_c \omega_p^2 / \omega(\omega^2 - \omega_c^2)$, and $\epsilon_{zz} = \epsilon_L (1 - \omega_p^2/\omega^2)$, and ϵ_L, ω_p, and ω_c are the background dielectric constant, plasma frequency, and cyclotron frequency, respectively, of the medium under consideration. The nontrivial solution of Eq. (2) is subject to the condition

$$-q_z^2 = \alpha_\pm^2 = \frac{1}{2\epsilon_{zz}} \{ (\epsilon_{xx} + \epsilon_{zz}) q_y^2 - 2 q_0^2 \epsilon_{xx} \epsilon_{zz} \pm [(\epsilon_{xx} - \epsilon_{zz})^2 q_y^4 + 4 (q_y^2 - q_0^2 \epsilon_{zz}) q_0^2 \epsilon_{xy}^2 \epsilon_{zz}]^{1/2} \} . \tag{3}$$

We write the field solutions in the two media as follows:

$$\mathbf{E}(\mathbf{r}, t) = \mathbf{E}(z) e^{i(q_y y - \omega t)} , \tag{4}$$

where $\mathbf{E}(z)$ for regions A and B are given by

$$\mathbf{E}_A(z) = \mathbf{E}_{1A} e^{\alpha_{A+} z} + \mathbf{E}_{2A} e^{-\alpha_{A+} z} + \mathbf{E}_{3A} e^{\alpha_{A-} z} + \mathbf{E}_{4A} e^{-\alpha_{A-} z} \tag{5}$$

and

$$\mathbf{E}_B(z) = \mathbf{E}_{1B} e^{\alpha_{B+} z} + \mathbf{E}_{2B} e^{-\alpha_{B+} z} + \mathbf{E}_{3B} e^{\alpha_{B-} z} + \mathbf{E}_{4B} e^{-\alpha_{B-} z} . \tag{6}$$

Analogous equations can be written for the magnetic field variable **B** in the respective regions.

Since the superlattice structure, Fig. 1, is periodic in the z direction, we want to synthesize the basic solutions, Eqs. (5) and (6), in the form of Bloch waves, so that the proper boundary conditions are satisfied at each interface. For this purpose, we invoke the following constitutive condition:

$$E_{A,B;n} = e^{ikd} E_{A,B;n-1} , \tag{7}$$

where $|k| \le \pi/d$. This equation is an exact analogue of the Bloch theorem for the electric fields associated with the magnetoplasmons of a periodic structure. As such, for any integer n, $E(z + nd) = e^{iknd} E(z)$; n labels the number of the cell. Here k is the wave vector that will ultimately enter the dispersion relation of the collective excitations of the superlattice.

The standard electromagnetic boundary conditions are the continuity of the tangential electric and magnetic field components: E_x, B_x, E_y, and B_y. The use of Maxwell's curl field equations and Eq. (2) enables one to write E_y, B_y, and B_x in terms of E_x in the respective regions. This considerably reduces the number of unknows involved. As such, the use of Eq. (7) along with the boundary conditions yields the following relations:

At $z = nd + d_A$,

$$E_{1A} e^{\alpha_{A+} d_A} + E_{2A} e^{-\alpha_{A+} d_A} + E_{3A} e^{\alpha_{A-} d_A} + E_{4A} e^{-\alpha_{A-} d_A} = E_{1B} + E_{2B} + E_{3B} + E_{4B} , \tag{8}$$

$$A_1 (E_{1A} e^{\alpha_{A+} d_A} + E_{2A} e^{-\alpha_{A+} d_A}) + A_2 (E_{3A} e^{\alpha_{A-} d_A} + E_{4A} e^{-\alpha_{A-} d_A}) = B_1 (E_{1B} + E_{2B}) + B_2 (E_{3B} + E_{4B}) , \tag{9}$$

$$\alpha_{A+} A_3 (E_{1A} e^{\alpha_{A+} d_A} - E_{2A} e^{-\alpha_{A+} d_A}) + \alpha_{A-} A_4 (E_{3A} e^{\alpha_{A-} d_A} - E_{4A} e^{-\alpha_{A-} d_A}) = \alpha_{B+} B_3 (E_{1B} - E_{2B}) + \alpha_{B-} B_4 (E_{3B} - E_{4B}) , \tag{10}$$

$$\alpha_{A+}(E_{1A}e^{\alpha_{A+}d_A}-E_{2A}e^{-\alpha_{A+}d_A})+\alpha_{A-}(E_{3A}e^{\alpha_{A-}d_A}-E_{4A}e^{-\alpha_{A-}d_A})=\alpha_{B+}(E_{1B}-E_{2B})+\alpha_{B-}(E_{3B}-E_{4B})\ ; \tag{11}$$

at $z=nd$,

$$E_{1A}+E_{2A}+E_{3A}+E_{4A}=e^{-iQ}[E_{1B}e^{\alpha_{B+}d_B}+E_{2B}e^{-\alpha_{B+}d_B}+E_{3B}e^{\alpha_{B-}d_B}+E_{4B}e^{-\alpha_{B-}d_B}]\ , \tag{12}$$

$$A_1(E_{1A}+E_{2A})+A_2(E_{3A}+E_{4A})=e^{-iQ}[B_1(E_{1B}e^{\alpha_{B+}d_B}+E_{2B}e^{-\alpha_{B+}d_B})+B_2(E_{3B}e^{\alpha_{B-}d_B}+E_{4B}e^{-\alpha_{B-}d_B})]\ , \tag{13}$$

$$\alpha_{A+}A_3(E_{1A}-E_{2A})+\alpha_{A-}A_4(E_{3A}-E_{4A})$$
$$=e^{-iQ}[\alpha_{B+}B_3(E_{1B}e^{\alpha_{B+}d_B}-E_{2B}e^{-\alpha_{B+}d_B})+\alpha_{B-}B_4(E_{3B}e^{\alpha_{B-}d_B}-E_{4B}e^{-\alpha_{B-}d_B})]\ , \tag{14}$$

$$\alpha_{A+}(E_{1A}-E_{2A})+\alpha_{A-}(E_{3A}-E_{4A})=e^{-iQ}[\alpha_{B+}(E_{1B}e^{\alpha_{B+}d_B}-E_{2B}e^{-\alpha_{B+}d_B})+\alpha_{B-}(E_{3B}e^{\alpha_{B-}d_b}-E_{4B}e^{-\alpha_{B-}d_B})]\ , \tag{15}$$

where

$$j_1=\frac{k_j^2-\alpha_{j+}^2}{q_0^2\epsilon_{xy}^j},\quad j_2=\frac{k_j^2-\alpha_{j-}^2}{q_0^2\epsilon_{xy}^j}\ , \tag{16a}$$

$$j_3=\frac{\epsilon_{zz}^j(k_j^2-\alpha_{j+}^2)}{\epsilon_{xy}^j(q_y^2-q_0^2\epsilon_{zz}^j)},\quad j_4=\frac{\epsilon_{zz}^j}{\epsilon_{xy}^j}\frac{(k_j^2-\alpha_{j-}^2)}{(q_y^2-q_0^2\epsilon_{zz}^j)}\ , \tag{16b}$$

$$k_j^2=q_y^2-q_0^2\epsilon_{xx}^j,\quad j\equiv A,B \tag{16c}$$

and Q $(=kd)$ is a dimensionless Bloch wave vector. The quantities $\alpha_{A\pm}$ and $\alpha_{B\pm}$ refer to the decay constants of the fields into the respective media. We thus obtain Eqs. (8)–(15) in terms of eight unknown coefficients—E_{1A}, E_{2A}, E_{3A}, E_{4A}, E_{1B}, E_{2B}, E_{3B}, and E_{4B}. Eliminating E_{1B}, E_{2B}, E_{3B}, and E_{4B} from these equations yields

$$(P_1+Q_1)(e^{B_++A_+}-e^{iQ})E_{1A}+(P_1-Q_1)(e^{B_+-A_+}-e^{iQ})E_{2A}$$
$$+(R_1+S_1)(e^{B_++A_-}-e^{iQ})E_{3A}+(R_1-S_1)(e^{B_+-A_-}-e^{iQ})E_{4A}=0\ , \tag{17}$$

$$(P_1-Q_1)(e^{-B_++A_+}-e^{iQ})E_{1A}+(P_1+Q_1)(e^{-B_+-A_+}-e^{iQ})E_{2A}$$
$$+(R_1-S_1)(e^{-B_++A_-}-e^{iQ})E_{3A}+(R_1+S_1)(e^{-B_+-A_-}-e^{iQ})E_{4A}=0\ , \tag{18}$$

$$(P_2+Q_2)(e^{B_-+A_+}-e^{iQ})E_{1A}+(P_2-Q_2)(e^{B_--A_+}-e^{iQ})E_{2A}$$
$$+(R_2+S_2)(e^{B_-+A_-}-e^{iQ})E_{3A}+(R_2-S_2)(e^{B_--A_-}-e^{iQ})E_{4A}=0\ , \tag{19}$$

$$(P_2-Q_2)(e^{-B_-+A_+}-e^{iQ})E_{1A}+(P_2+Q_2)(e^{-B_--A_+}-e^{iQ})E_{2A}$$
$$+(R_2-S_2)(e^{-B_-+A_-}-e^{iQ})E_{3A}+(R_2+S_2)(e^{-B_--A_-}-e^{iQ})E_{4A}=0\ , \tag{20}$$

where

$$P_1=(A_1-B_2)(B_3-B_4)\alpha_{B+},\quad P_2=(A_1-B_1)(B_3-B_4)\alpha_{B-},$$
$$Q_1=(A_3-B_4)(B_1-B_2)\alpha_{A+},\quad Q_2=(A_3-B_3)(B_1-B_2)\alpha_{A+},$$
$$R_1=(A_2-B_2)(B_3-B_4)\alpha_{B+},\quad R_2=(A_2-B_1)(B_3-B_4)\alpha_{B-},$$
$$S_1=(A_4-B_4)(B_1-B_2)\alpha_{A-},\quad S_2=(A_4-B_3)(B_1-B_2)\alpha_{A-},$$

and $B_\pm=\alpha_{B\pm}d_B$, $A_\pm=\alpha_{A\pm}d_A$. As such, we have four homogeneous equations, Eqs. (17)–(20), in terms of four unknown coefficients—$E_{iA}(i=1,2,3,4)$. Setting the appropriate determinant to zero yields an (implicit) general dispersion relation for the collective (bulk) modes for the magnetoplasmons of the superlattice system. This reads

$$\begin{vmatrix}(P_1+Q_1)(e^{B_++A_+}-e^{iQ}) & (P_1-Q_1)(e^{B_+-A_+}-e^{iQ}) & (R_1+S_1)(e^{B_++A_-}-e^{iQ}) & (R_1-S_1)(e^{B_+-A_-}-e^{iQ})\\ (P_1-Q_1)(e^{-B_++A_+}-e^{iQ}) & (P_1+Q_1)(e^{-B_+-A_+}-e^{iQ}) & (R_1-S_1)(e^{-B_++A_-}-e^{iQ}) & (R_1+S_1)(e^{-B_+-A_-}-e^{iQ})\\ (P_2+Q_2)(e^{B_-+A_+}-e^{iQ}) & (P_2-Q_2)(e^{B_--A_+}-e^{iQ}) & (R_2+S_2)(e^{B_-+A_-}-e^{iQ}) & (R_2-S_2)(e^{B_--A_-}-e^{iQ})\\ (P_2-Q_2)(e^{-B_-+A_+}-e^{iQ}) & (P_2+Q_2)(e^{-B_--A_+}-e^{iQ}) & (R_2-S_2)(e^{-B_-+A_-}-e^{iQ}) & (R_2+S_2)(e^{-B_--A_-}-e^{iQ})\end{vmatrix}=0\ . \tag{21}$$

Equation (21) is the general dispersion relation for the collective excitations to include the effect of retardation and an external magnetic field parallel to the superlattice axis (taken to be the $\hat{z}$ axis). For fixed q_y, this yields the frequency (ω) bands when ω is plotted versus Q ($=kd$).

It is worthwhile mentioning that the dispersion relation, Eq. (21), has been checked by imposing the limits $d_A \to \infty$, $d_B \to \infty$, and treating the semi-infinite layer A (or B) as an insulator characterized by frequency-independent dielectric constant ϵ_A (or ϵ_B). It is found that within these special limits our general dispersion relation reproduces exactly the proper results previously reported for a surface ($\mathbf{B}_0 \neq \mathbf{0}$).[16]

B. Truncated superlattices

Now let the superlattice in Fig. 1 be truncated at $z=0$ such that the medium in the region $z \le 0$ is an insulator with a dieletric tensor ϵ_C being diagonal. We seek solutions to Maxwell's equations in which the fields are localized at each interface of the superlattice and at $z=0$, between the insulator and the first layer of the superlattice. The solutions at $z=0$ are equivalent to those at $z=nd$; with $n=0$. We match E_x, E_y, B_x, and B_y field components at $z=0$. The result is

$$E_{1A}+E_{2A}+E_{3A}+E_{4A}=E_{xC} , \tag{22}$$

$$A_1(E_{1A}+E_{2A})+A_2(E_{3A}+E_{4A})=E_{yC} , \tag{23}$$

$$\alpha_{A+}A_3(E_{1A}-E_{2A})+\alpha_{A-}A_4(E_{3A}-E_{4A})=q_0^2\frac{\epsilon_C}{\alpha_C}E_{yC} , \tag{24}$$

$$\alpha_{A+}(E_{1A}-E_{2A})+\alpha_{A-}(E_{3A}-E_{4A})=\alpha_C E_{xC} , \tag{25}$$

where $\alpha_C=q_y^2-q_0^2\epsilon_C$ describes the decay of the field into the dielectric ($z \le 0$). Eliminating E_{xC} from Eqs. (22) and (25), and E_{yC} from Eqs. (23) and (24), yields

$$y_1E_{1A}+y_2E_{2A}+y_3E_{3A}+y_4E_{4A}=0 , \tag{26}$$

$$z_1E_{1A}+z_2E_{2A}+z_3E_{3A}+z_4E_{4A}=0 , \tag{27}$$

where

$$y_1=\alpha_C-\alpha_{A+}, \quad z_1=q_0^2\frac{\epsilon_C}{\alpha_C}A_1-\alpha_{A+}A_3 ,$$

$$y_2=\alpha_C+\alpha_{A+}, \quad z_2=q_0^2\frac{\epsilon_C}{\alpha_C}A_1+\alpha_{A+}A_3 ,$$

$$y_3=\alpha_C-\alpha_{A-}, \quad z_3=q_0^2\frac{\epsilon_C}{\alpha_C}A_2-\alpha_{A-}A_4 ,$$

$$y_4=\alpha_C+\alpha_{A-}, \quad z_4=q_0^2\frac{\epsilon_C}{\alpha_C}A_2+\alpha_{A-}A_4 .$$

Since the surface modes are characterized by the exponentially decaying fields, we use the condition $E(z+nd)=e^{-\beta nd}E(z)$ instead of the Bloch condition stated in the text following Eq. (7); $\beta=-ik$. Equation (21) still holds good if it is modified by replacing $\cos(Q)$ by $\cosh(\lambda)$; $\lambda=\beta d$.

In order to explicitly determine the collective (surface) excitations of a truncated superlattice, we modify Eqs. (17)–(20) by replacing Q by $i\lambda$. The result is

$$(P_1+Q_1)(e^{B_++A_+}-e^{-\lambda})E_{1A}+(P_1-Q_1)(e^{B_+-A_+}-e^{-\lambda})E_{2A}+(R_1+S_1)(e^{B_++A_-}-e^{-\lambda})E_{3A} +(R_1-S_1)(e^{B_+-A_-}-e^{-\lambda})E_{4A}=0 , \tag{28}$$

$$(P_1-Q_1)(e^{-B_++A_+}-e^{-\lambda})E_{1A}+(P_1+Q_1)(e^{-B_+-A_+}-e^{-\lambda})E_{2A}+(R_1-S_1)(e^{-B_++A_-}-e^{-\lambda})E_{3A} +(R_1+S_1)(e^{-B_+-A_-}-e^{-\lambda})E_{4A}=0 , \tag{29}$$

$$(P_2+Q_2)(e^{B_-+A_+}-e^{-\lambda})E_{1A}+(P_2-Q_2)(e^{B_--A_+}-e^{-\lambda})E_{2A}+(R_2+S_2)(e^{B_-+A_-}-e^{-\lambda})E_{3A} +(R_2-S_2)(e^{B_--A_-}-e^{-\lambda})E_{4A}=0 , \tag{30}$$

$$(P_2-Q_2)(e^{-B_-+A_+}-e^{-\lambda})E_{1A}+(P_2+Q_2)(e^{-B_--A_+}-e^{-\lambda})E_{2A}+(R_2-S_2)(e^{-B_-+A_-}-e^{-\lambda})E_{3A} +(R_2+S_2)(e^{-B_--A_-}-e^{-\lambda})E_{4A}=0 . \tag{31}$$

Next, the condition that Eqs. (26)–(29) have nontrivial solutions leaves us with

$$a_1e^{-2\lambda}-b_1e^{-\lambda}+c_1=0 , \tag{32}$$

where

$$a_1=[(P_1+Q_1)^2-(P_1-Q_1)^2](y_3z_4-y_4z_3)+[(R_1+S_1)^2-(R_1-S_1)^2](y_1z_2-y_2z_1)$$
$$+[(P_1-Q_1)(R_1+S_1)-(P_1+Q_1)(R_1-S_1)](y_2z_4-y_4z_2)$$
$$+[(P_1+Q_1)(R_1+S_1)-(P_1-Q_1)(R_1-S_1)](y_2z_3-y_3z_2)$$
$$+[(P_1-Q_1)(R_1-S_1)-(P_1+Q_1)(R_1+S_1)](y_1z_4-y_4z_1)$$
$$+[(P_1+Q_1)(R_1-S_1)-(P_1-Q_1)(R_1+S_1)](y_1z_3-y_3z_1)\ ,$$

$$c_1=[(P_1+Q_1)^2-(P_1-Q_1)^2](y_3z_4-y_4z_3)+[(R_1+S_1)^2-(R_1-S_1)^2](y_1z_2-y_2z_1)$$
$$+[(P_1-Q_1)(R_1+S_1)-(P_1+Q_1)(R_1-S_1)](y_2z_4-y_4z_2)e^{A_++A_-}$$
$$+[(P_1+Q_1)(R_1+S_1)-(P_1-Q_1)(R_1-S_1)](y_2z_3-y_3z_2)e^{A_+-A_-}$$
$$+[(P_1-Q_1)(R_1-S_1)-(P_1+Q_1)(R_1+S_1)](y_1z_4-y_4z_1)e^{-A_++A_-}$$
$$+[(P_1+Q_1)(R_1-S_1)-(P_1-Q_1)(R_1+S_1)](y_1z_3-y_3z_1)e^{-A_+-A_-}\ ,$$

$$b_1=[(P_1+Q_1)^2(e^{B_++A_+}+e^{-B_+-A_+})-(P_1-Q_1)^2(e^{B_+-A_+}+e^{-B_++A_+})](y_3z_4-y_4z_3)$$
$$+[(R_1+S_1)^2(e^{B_++A_-}+e^{-B_+-A_-})-(R_1-S_1)^2(e^{B_+-A_-}+e^{-B_++A_-})](y_1z_2-y_2z_1)$$
$$+[(P_1-Q_1)(R_1+S_1)(e^{B_++A_-}+e^{-B_++A_+})-(P_1+Q_1)(R_1-S_1)(e^{B_++A_+}+e^{-B_++A_-})](y_2z_4-y_4z_2)$$
$$+[(P_1+Q_1)(R_1+S_1)(e^{B_++A_+}+e^{-B_+-A_-})-(P_1-Q_1)(R_1-S_1)(e^{B_+-A_-}+e^{-B_++A_+})](y_2z_3-y_3z_2)$$
$$+[(P_1-Q_1)(R_1-S_1)(e^{B_+-A_+}+e^{-B_++A_-})-(P_1+Q_1)(R_1+S_1)(e^{B_++A_-}+e^{-B_+-A_+})](y_1z_4-y_4z_1)$$
$$+[(P_1+Q_1)(R_1-S_1)(e^{B_+-A_-}+e^{-B_+-A_+})-(P_1-Q_1)(R_1+S_1)(e^{B_+-A_+}+e^{-B_+-A_-})](y_1z_3-y_3z_1)\ .$$

Similarly, the condition that Eqs. (26), (27), (30), and (31) have nontrivial solutions takes the form

$$a_2e^{-2\lambda}-b_2e^{-\lambda}+c_2=0\ , \tag{33}$$

where

$$a_2=[(P_2+Q_2)^2-(P_2-Q_2)^2](y_3z_4-y_4z_3)+[(R_2+S_2)^2-(R_2-S_2)^2](y_1z_2-y_2z_1)$$
$$+[(P_2-Q_2)(R_2+S_2)-(P_2+Q_2)(R_2-S_2)](y_2z_4-y_4z_2)$$
$$+[(P_2+Q_2)(R_2+S_2)-(P_2-Q_2)(R_2-S_2)](y_2z_3-y_3z_2)$$
$$+[(P_2-Q_2)(R_2-S_2)-(P_2+Q_2)(R_2+S_2)](y_1z_4-y_4z_1)$$
$$+[(P_2+Q_2)(R_2-S_2)-(P_2-Q_2)(R_2+S_2)](y_1z_3-y_3z_1)\ ,$$

$$c_2=[(P_2+Q_2)^2-(P_2-Q_2)^2](y_3z_4-y_4z_3)+[(R_2+S_2)^2-(R_2-S_2)^2](y_1z_2-y_2z_1)$$
$$+[(P_2-Q_2)(R_2+S_2)-(P_2+Q_2)(R_2-S_2)](y_2z_4-y_4z_2)e^{A_++A_-}$$
$$+[(P_2+Q_2)(R_2+S_2)-(P_2-Q_2)(R_2-S_2)](y_2z_3-y_3z_2)e^{A_+-A_-}$$
$$+[(P_2-Q_2)(R_2-S_2)-(P_2+Q_2)(R_2+S_2)](y_1z_4-y_4z_1)e^{-A_++A_-}$$
$$+[(P_2+Q_2)(R_2-S_2)-(P_2-Q_2)(R_2+S_2)](y_1z_3-y_3z_1)e^{-A_+-A_-}\ ,$$

$$b_2=[(P_2+Q_2)^2(e^{B_-+A_+}+e^{-B_--A_+})-(P_2-Q_2)^2(e^{B_--A_+}+e^{-B_-+A_+})](y_3z_4-y_4z_3)$$
$$+[(R_2+S_2)^2(e^{B_-+A_-}+e^{-B_--A_-})-(R_2-S_2)^2(e^{B_--A_-}+e^{-B_-+A_-})](y_1z_2-y_2z_1)$$
$$+[(P_2-Q_2)(R_2+S_2)(e^{B_-+A_-}+e^{-B_-+A_+})-(P_2+Q_2)(R_2-S_2)(e^{B_-+A_+}+e^{-B_-+A_-})](y_2z_4-y_4z_2)$$
$$+[(P_2+Q_2)(R_2+S_2)(e^{B_-+A_+}+e^{-B_--A_-})-(P_2-Q_2)(R_2-S_2)(e^{B_--A_-}+e^{-B_-+A_+})](y_2z_3-y_3z_2)$$
$$+[(P_2-Q_2)(R_2-S_2)(e^{B_--A_+}+e^{-B_-+A_-})-(P_2+Q_2)(R_2+S_1)(e^{B_-+A_-}+e^{-B_--A_+})](y_1z_4-y_4z_1)$$
$$+[(P_2+Q_2)(R_2-S_2)(e^{B_--A_-}+e^{-B_--A_+})-(P_2-Q_2)(R_2+S_2)(e^{B_--A_+}+e^{-B_--A_-})](y_1z_3-y_3z_1)\ .$$

The general dispersion relation for the magnetoplasma polaritons in the truncated superlattice system is obtained by eliminating $\exp(-\lambda)$ from Eqs. (32) and (33). The result is

$$(a_1 b_2 - a_2 b_1)(b_1 c_2 - b_2 c_1) - (c_1 a_2 - c_2 a_1)^2 = 0 \ . \quad (34)$$

It is found that a careful analytic diagnosis within the special limits, just as those imposed on Eq. (21), leads our implicit dispersion relation, Eq. (34), to reproduce the proper results ($\mathbf{B}_0 \neq 0$).[16]

III. NUMERICAL EXAMPLES

We have carried out an extensive numerical calculation of the magnetoplasma (bulk and surface) excitations, using the analytical expressions, Eqs. (21) and (34), for the dispersion relations of the superlattice structure in the local theory with retardation. For this purpose, we have taken the background dielectric constant $\epsilon_L = 13.13$ and ignored the damping and optical polar phonons. As such our numerical results are more appropriate for superlattice structure comprised of semiconductors rather than metals. The case of metallic superlattices in the presence of an applied magnetic field in the Voigt geometry was recently studied by Wallis *et al.*[13]

In general, we have performed the computation in the situation where both constituent layers contain free charge carriers and are characterized by the frequency- and magnetic-field-dependent dielectric functions in the local approximation. We have plotted our numerical results for several illustrative cases in terms of the dimensionless frequency $\xi = \omega / \omega_{pA}$, the dimensionless wave vector $\zeta = c q_y / \omega_{pA}$, and the dimensionless layer thicknesses $\delta_A = \omega_{pA} d_A / c$ and $\delta_B = \omega_{pA} d_B / c$. In order to provide the comparison, we have presented the results both with and without[15] an applied magnetic field. Since the existence of the surface magnetoplasma polaritons depends upon the relative magnitude of the layer thicknesses, we have considered several representative cases. We have also shown the effect of magnetic field variation.

Before we present the numerical results it is instructive to consider the possibilities of the propagating plasma modes comprising the bulk and surface excitations. In the present (perpendicular) configuration *four* different kinds of modes can be allowed to propagate. Depending upon the spectral range in the frequency–wave-vector plane the following possibilities may arise: (i) α_{i+} and α_{i-} are both real and positive, (ii) α_{i+} and α_{i-} are both pure imaginary, (iii) α_{i+} is real and α_{i-} is pure imaginary, or vice versa, and (iv) α_{i+} and α_{i-} are complex conjugates of each other. We will term the magnetoplasma modes corresponding to the above-mentioned scheme as surface-polariton (SP) modes, bulk modes, pseudosurface (PS) modes, and generalized complex (GC) modes, respectively. This classification will help us understand the behavior of electromagnetic modes in the specific spectral region with respect to both of the consituent layers ($i = A, B$). As mentioned above, since we are interested in the magnetoplasma excitations localized at the interfaces and decaying exponentially away from them, the SP and the GC (with positive real parts much greater than their imaginary parts) modes are more pertinent than the bulk and the PS modes. Remember, the aforesaid nomenclature of the modes requires the same nature of the decay constants ($\alpha_{i\pm}$) in both of the material layers.

The material parameters used in the present computation are $\epsilon_L (= \epsilon_{LA} = \epsilon_{LB}) = 13.13$; $\epsilon_C = 1.0$; $\omega_{pB} = 0.5\omega_{pA}$; $\omega_{cA} = 0.25\omega_{pA}$, $0.5\omega_{pA}$; $\delta_A = 1.0$; $\delta_B = 0.5, 1.0, 2.0$. That is to say that we have studied the dispersion relations as a function of the magnitude of an applied magnetic field ($\mathbf{B}_0$) and the thickness of the B layers. For zero magnetic field, we have used Eqs. (23) and (31) of Ref. 15, respectively, for the bulk and surface excitations. Although the mathematical complexity of the dispersion relations prevents us from making a detailed analytical diagnosis, we will later discuss some approximate analysis in the nonretarded limit ($c \to \infty$) to establish some consistency with the numerical results, both for zero- and nonzero-magnetic-field cases.

A. $\delta_A = 1.0, \delta_B = 0.5$

In Figs. 2, 3, and 4, we present the dispersion curves for bulk and surface excitations for $\mathbf{B}_0 = 0$, $\omega_c (= \omega_{cB} = \omega_{cA}) = 0.25\omega_{pA}$, and $\omega_c = 0.5\omega_{pA}$, respectively. In the case of zero magnetic field, we find two bulk bands separated by a gap for an infinite superlattice. In the gap lies the mode for a truncated superlattice. The existence of the upper SP mode is implied by the fact that $\epsilon_L / \epsilon_C > 1$. In the case that $\epsilon_L / \epsilon_C < 1$, this SP mode will fall below the lower bulk band. Note that there is no bulk band existing below ω_{pB}.

For nonzero magnetic field, $\omega_c = 0.25\omega_{pA}$ (Fig. 3), we find that there are no bona fide bulk and/or surface modes below ω_c. This is the PS wave region where we

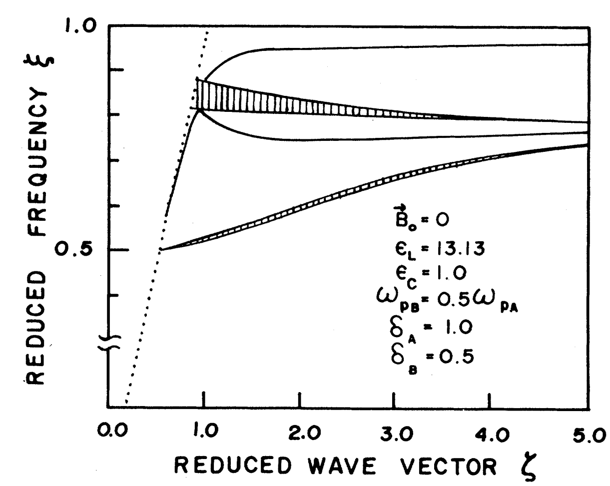

FIG. 2. Dispersion curves for the surface polaritons of the truncated superlattice and the allowed bulk bands (cross-hatched regions) of the infinite superlattice in the absence of a magnetic field, with $\delta_B = 0.5\delta_A$. The parameters used are listed in the figure. $\alpha_c = 0$ is the light line.

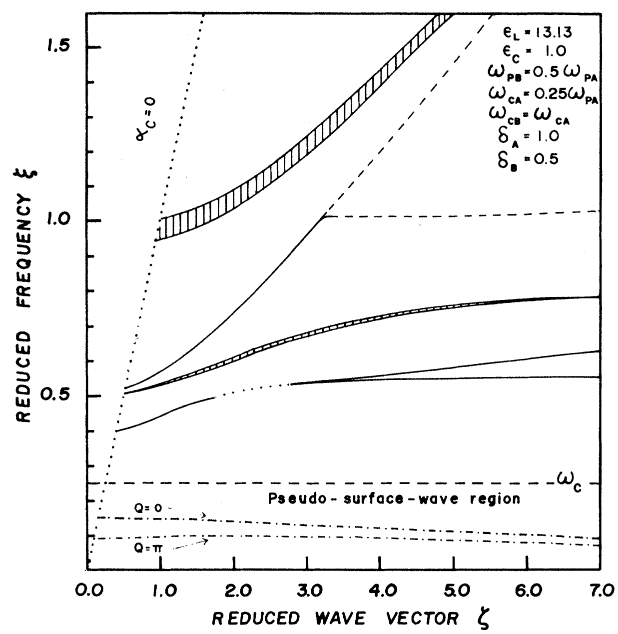

FIG. 3. Dispersion curves for the surface polaritons of the truncated superlattice and the allowed bulk bands (cross-hatched regions) of the infinite superlattice in the presence of a magnetic field, with $\omega_c = 0.25\omega_{pA}$ and $\delta_B = 0.5\delta_A$.

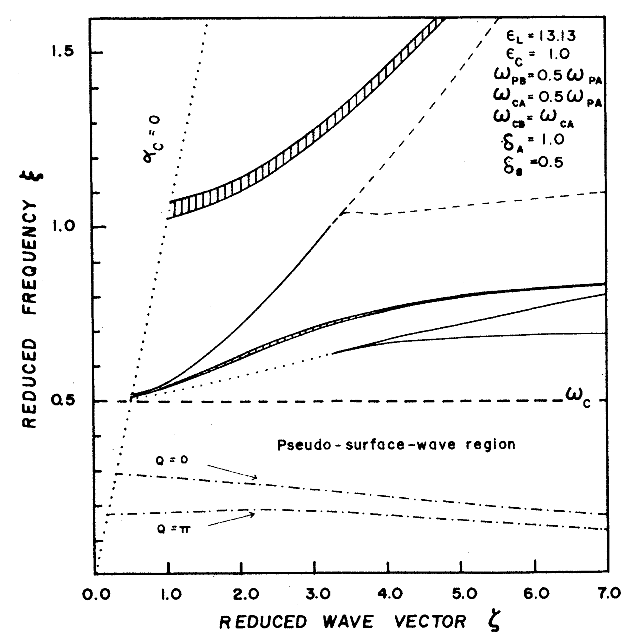

FIG. 4. Dispersion curves for the surface polaritons of the truncated superlattice and the allowed bulk bands (cross-hatched regions) of the infinite superlattice in the presence of a magnetic field with $\omega_c = 0.5\omega_{pA}$ and $\delta_B = 0.5\delta_A$.

have shown (dashed-dotted curves) a bulk band whose both edges reveal the frequency (ξ) decreasing with increasing wave vector (ζ). These are the modes characterized by $\mathrm{Re}\alpha_{i+}$ being comparable or smaller (in magnitude) than $\mathrm{Im}\alpha_{i-}$. Although we have shown the effect of $\mathbf{B}_0$ and relative thickness of the layers on these modes (in the PS wave region) in each case, *we will not discuss them further.* The lowest bona fide mode is the pure SP mode starting at $\omega \simeq 0.4\omega_{pA}$. This mode propagates until it approaches ω_{pB}; just above ω_{pB} the decay constants $\alpha_{B\pm}$ assume the complex-conjugate values with their $\mathrm{Re}\alpha_{B\pm} > \mathrm{Im}\alpha_{B\pm}$. This situation prevails from $\zeta \simeq 1.8$ to $\zeta \simeq 2.8$. At $\zeta \simeq 2.8$ this mode again attains its pure SP mode character and splits into two, shown by a fork in the figure. Interestingly, the lower branch of this mode is found to have an asymptotic limit ω_{HB} (the hybrid plasmon-cyclotron frequency for B layer). The bona fide (lower) bulk band starts at $\xi \simeq 0.5084$ ($Q = \pi$) and 0.5094 ($Q = 0$). Above this bulk band at $\xi \simeq 0.5217$ starts a pure SP mode which propagates with increasing frequency until it reaches ω_{pA}; just above ω_{pA} it also changes its character from SP to GC modes and splits into two branches (shown by a fork with dashed lines). We note that the latter (GC) modes are characterized, over most of the wave-vector range, by the $\mathrm{Re}\alpha_{i\pm} \gg \mathrm{Im}\alpha_{i\pm}$. The lower branch shows both positive and negative group velocities between $\zeta \simeq 3.25$ and $\zeta \simeq 3.60$. The upper (bona fide) bulk band starts in the vicinity of ω_{pA} with widely separated edges which come closer with increasing ζ. It is interesting to note that none of the SP modes emerges from or merges into any of the two bulk bands in the whole ξ-ζ plane shown in the figure.

The situation with $\omega_c = 0.5\omega_{pA}$ is depicted in Fig. 4. The lowest SP mode, characterized by real $\alpha_{A\pm}$ and complex-conjugate $\alpha_{B\pm}$ (with $\mathrm{Re}\alpha_{B\pm} > \mathrm{Im}\alpha_{B\pm}$), starts at $\xi \simeq 0.5086$, increases monotonously until it reaches $\zeta \simeq 3.3$, where it changes it behavior to pure SP mode and splits into two branches (shown by a fork). The lower branch goes to the asymptotic limit ω_{HB} and the upper one still increases with increasing ζ. The lower bulk band starts at the light line just above this lower SP mode. The upper SP mode starts at $\xi \simeq 0.5127$ from the light line in the gap between two bulk bands, with its frequency increasing with ζ until it reaches ω_{pA}, where it changes its character from SP to (bona fide) GC modes, and then at $\zeta \simeq 3.4$ splits into two branches, just as in Fig. 3. The lower branch reveals both negative and positive group velocities in the range between $\zeta \simeq 3.4$ and $\zeta \simeq 4.19$. Note that $\zeta \simeq 4.19$ for this mode, with $\xi \simeq 1.0404$, is the point characterized by $\epsilon_{zz}^{A} = 1$ where the lower (split) mode changes the sign of its group velocity from negative to positive. It is worth mentioning that the frequency given by $\epsilon_{zz}^{A} = 1$ where the group velocity changes its sign, in this case, is a sheer coincidence and a consequence of the choice of the material parameters, but is not a fact independent of the value of $\mathbf{B}_0$. However, the split of the upper SP mode, just above ω_{pA}, in the gap between two bulk bands seems to occur only above a certain value of $\mathbf{B}_0$. The effect of magnetic field results in the widening of the gap between the two bulk bands and a Zeeman-like splitting of the two SP modes at large wave vectors. Moreover, there is no SP mode occurring above the upper bulk band in the presence of an external magnetic field. This is because the decay constants $\alpha_{i\pm}$ there do not attain the values which fulfill the requirements of the bona fide SP modes.

B. $\delta_A = \delta_B = 1.0$

In this case of equal layer thicknesses the numerical results are plotted in Figs. 5, 6, and 7 for $\mathbf{B}_0 = 0$, $\omega_c = 0.25\omega_{pA}$, and $\omega_c = 0.5\omega_{pA}$, respectively. In the case of zero magnetic field (Fig. 5), we notice that the gap between the two bulk bands decreases as compared to that in Fig. 2, and the SP mode occurring in the gap does not exist at large ζ. In fact the existence of this mode, even at lower ζ, can be attributed to the retardation effect. In the nonretardation limit, for $\delta_A = \delta_B$, no gap occurs between two bulk bands and hence no SP mode. Furthermore, it is observed that while the upper SP mode above the upper bulk band remains almost intact, the frequency of the SP mode (in the gap) happens to decrease over almost the whole wave-vector range.

For nonzero magnetic field (Figs. 6 and 7) the significant features compared to the previous cases (Figs. 3 and 4) are as follows. The gap between the two bulk bands decreases, particularly at the lower wave vectors. This results in the reduction of the spatial separation between the SP mode (in the gap) and the lower bulk band near the starting points. In the case of the higher magnetic field (Fig. 7), the upper SP mode seems to merge with the lower bulk band in the range between $\zeta \simeq 0.5$ and $\zeta \simeq 1.15$. This is not so—actually the deviation is so small that it is difficult to discern it on the scale in Fig. 7. The slope of the third-lowest SP mode above ω_{pA} in the

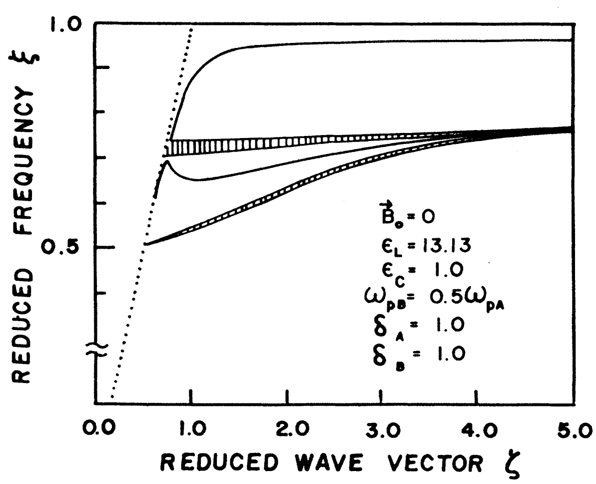

FIG. 5. Dispersion curves for the surface polaritons of the truncated superlattice and the allowed bulk bands (cross-hatched regions) of the infinite superlattice in the absence of a magnetic field, with $\delta_B = \delta_A$.

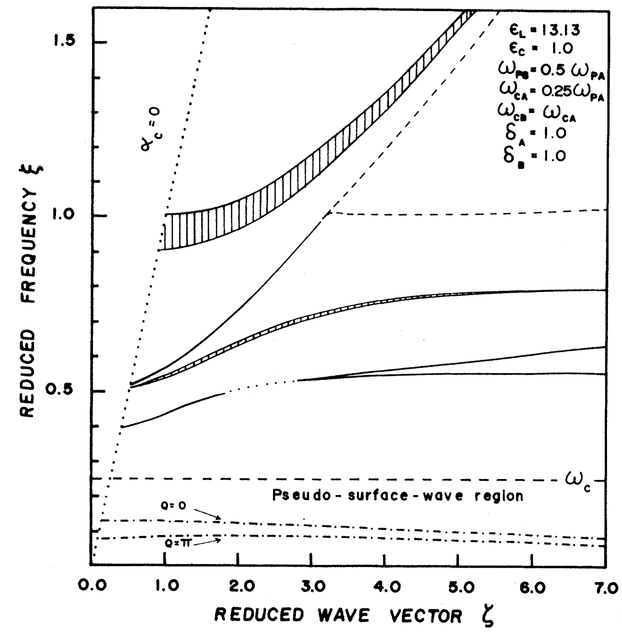

FIG. 6. Dispersion curves for the surface polaritons of the truncated superlattice and the allowed bulk bands (cross-hatched regions) of the infinite superlattice in the presence of a magnetic field, with $\omega_c = 0.25\omega_{pA}$ and $\delta_B = \delta_A$.

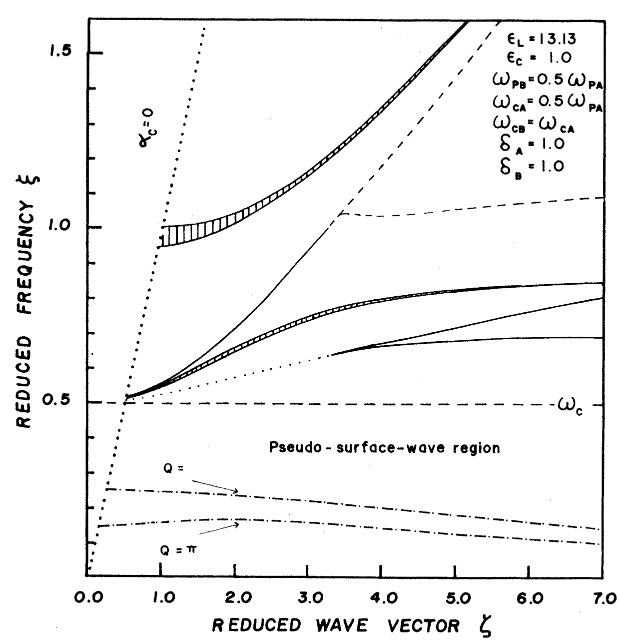

FIG. 7. Dispersion curves for the surface polaritons of the truncated superlattice and the allowed bulk bands (cross-hatched regions) of the infinite superlattice in the presence of a magnetic field, with $\omega_c = 0.5\omega_{pA}$ and $\delta_B = \delta_A$.

range where it shows both signs of group velocity has become clearer in the case of higher magnetic field. Apart from a very minute difference in the frequencies of the SP modes due to the variation of the relative thicknesses of the layers, the rest of the discussion related to Figs. 3 and 4 is still valid.

C. $\delta_A = 1.0, \delta_B = 2.0$

We now turn to the situation where the layer thickness of the denser medium (δ_A) is smaller than that of the less-dense medium (δ_B). The numerical results for $\mathbf{B}_0 = 0$, $\omega_c = 0.25\omega_{pA}$, and $\omega_c = 0.5\omega_{pA}$ are illustrated in Figs. 8, 9, and 10, respectively. In the absence of magnetic field (Fig. 8), the gap between the two bulk bands becomes smaller as compared to that seen in Fig. 5. The SP mode in the gap, and also the one occurring above the upper bulk band, starts at relatively low frequencies but reaches the same asymptotic limits as in Figs. 2 and 5. The SP mode in the gap loses its existence at considerably lower wave vectors and merges into the upper bulk band.

We now examine the situation for nonzero magnetic field. It is observed that increasing δ_B has resulted in lowering the upper bulk band and hence in reducing the gap as compared to the case of equal layer thicknesses. Note that while the bulk bands are seen to be affected considerably by change in the thickness of the B layer, the surface modes do not experience any *major* change with respect to their behavior in the whole ξ-ζ plane. It is worth mentioning that all parts of the SP modes, whether shown by dotted and/or dashed lines, are the bona fide and physically significant solutions. This remark is valid for all the nonzero-magnetic-field cases.

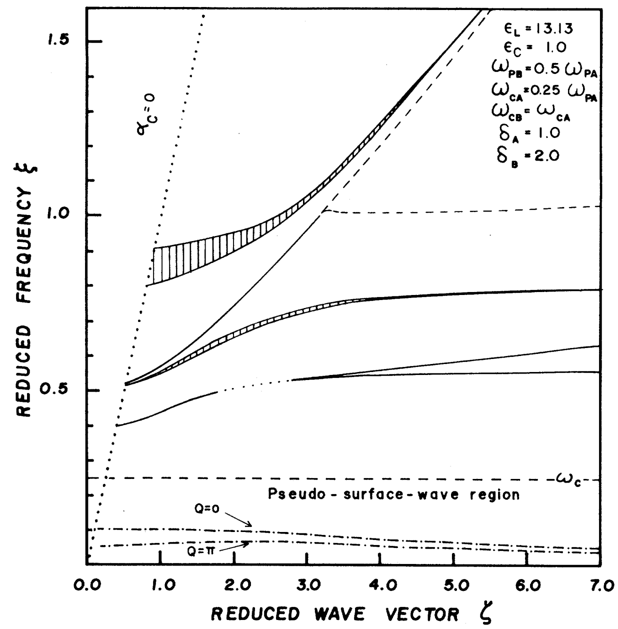

FIG. 9. Dispersion curves for the surface polaritons of the truncated superlattice and the allowed bulk bands (cross-hatched regions) of the infinite superlattice in the presence of a magnetic field, with $\omega_c = 0.25\omega_{pA}$ and $\delta_B = 2.0\delta_A$.

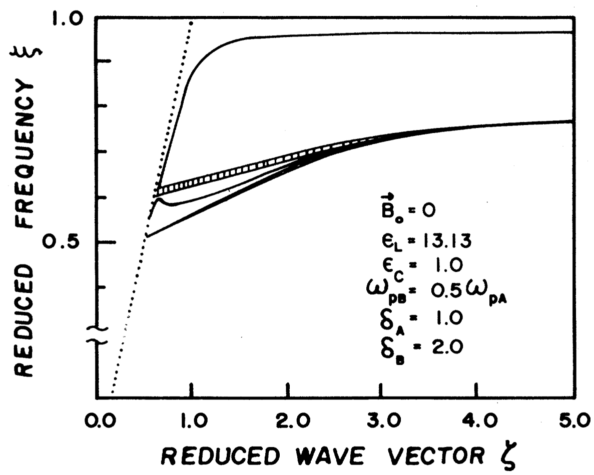

FIG. 8. Dispersion curves for the surface polaritons of the truncated superlattice and the allowed bulk bands (cross-hatched regions) of the infinite superlattice in the absence of a magnetic field, with $\delta_B = 2.0\delta_A$.

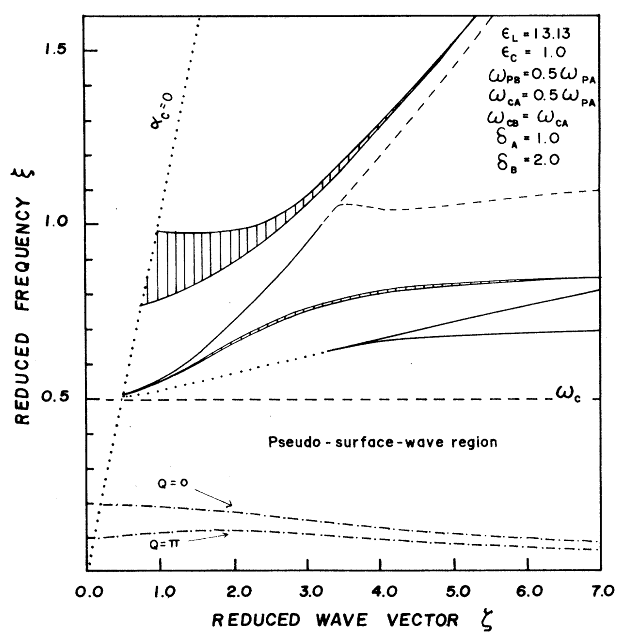

FIG. 10. Dispersion curves for the surface polaritons of the truncated superlattice and the allowed bulk bands (cross-hatched regions) of the infinite superlattice in the presence of a magnetic field, with $\omega_c = 0.5\omega_{pA}$ and $\delta_B = 2.0\delta_A$.

IV. DISCUSSION AND CONCLUSIONS

The different features exhibited by the numerical results can be understood, at least up to some extent, by some approximate analytical diagnosis. Let us recall our Eq. (23) from Ref. 15 for the dispersion relation of the collective (bulk) excitations for the $\mathbf{B}_0=0$ case. In the nonretardation limit ($c \rightarrow \infty$), this reduces to

$$\epsilon_A + \epsilon_B = 0 \ , \tag{35}$$

where $\epsilon_i(\omega)$ $[=\epsilon_L(1-\omega_{pi}^2/\omega^2)]$ is the frequency-dependent dielectric function for the ith layer ($i \equiv A,B$). Substituting the parameters used in the present calculations leads us to obtain $\xi \simeq 0.7906$. This is the frequency attained by the bulk bands in the asymptotic limit, as seen in Figs. 2, 5, and 8. Similarly, Eq. (31) in Ref. 15, which is the dispersion relation for the collective (surface) excitations for the zero magnetic field, in the nonretarded limit assumes the form

$$(\epsilon_A + \epsilon_B)(\epsilon_A + \epsilon_C)(\epsilon_B - \epsilon_C) = 0 \ , \tag{36}$$

where $\epsilon_C = 1$ is the frequency-independent dielectric constant of the insulator medium truncating the superlattice system at $z \leq 0$. Setting the first factor in Eq. (36) to zero gives us $\xi_1 \simeq 0.7906$. Similarly, setting the second factor to zero yields $\xi_2 \simeq 0.9639$. It can be easily seen that ξ_1 and ξ_2 are the asymptotic limits of SP modes, lying, respectively, in the gap and above the upper bulk band; see Figs. 2, 5, and 8.

In the case of nonzero magnetic field, our Eq. (21) in the nonretarded limit reduces to

$$\left\{ \left[\left[\frac{\epsilon_{xx}^A \epsilon_{zz}^A}{\epsilon_{xx}^B \epsilon_{zz}^B} \right]^{1/2} + \left[\frac{\epsilon_{xx}^B \epsilon_{zz}^B}{\epsilon_{xx}^A \epsilon_{zz}^A} \right]^{1/2} \right] \tanh(A'_+) \tanh(B'_+) + 2 \right\} - 2\cos(Q)\,\mathrm{sech}(A'_+)\,\mathrm{sech}(B'_+) = 0 \ , \tag{37}$$

where $J'_+ = (\epsilon_{xx}^i/\epsilon_{zz}^j)^{1/2} q_y d_j$, $j \equiv A,B$. Now taking $q_y \rightarrow \infty$ in Eq. (37) yields

$$(\epsilon_{xx}^A \epsilon_{zz}^A)^{1/2} + (\epsilon_{xx}^B \epsilon_{zz}^B)^{1/2} = 0 \ , \tag{38}$$

which is equivalent to

$$\xi^2 = \frac{1}{2} \left[1 + \frac{\omega_{pB}^2}{\omega_{pA}^2} + \frac{\omega_c^2}{\omega_{pA}^2} \right] . \tag{39}$$

Here ω_c $(=\omega_{cA} = \omega_{cB})$. Substituting in the parameters as used in the present computation, we obtain

$$\xi = \begin{cases} 0.81009 & \text{for } \omega_c/\omega_{pA} = 0.25 \\ 0.86603 & \text{for } \omega_c/\omega_{pA} = 0.5 . \end{cases} \tag{40}$$

As such, one can see the lower bulk bands approaching the asymptotic limits $\xi \simeq 0.81009$ (Figs. 3, 6, and 9) and $\xi \simeq 0.86603$ (Figs. 4, 7, and 10) for the respective values of the magnetic field. It should be pointed out that the mathematical complexity does not permit us to find any simple analytical explanation for the asymptotic limit approached by the lowest SP mode in the nonretardation limit for nonzero magnetic field.

In conclusion, we have studied the magnetoplasma (bulk and surface) polaritons in a truncated superlattice system in the presence of a transverse magnetic field. Although we have confined our attention to the case of a superlattice system comprised of two semiconducting layers, the theory quite clearly applies to the metallic superlattices as well; just by taking the background dielectric constant ϵ_L equal to unity. We have presented various illustrative numerical examples where one can examine the effect of the variation of the magnetic field as well as that of the variation of layer thickness of the less-dense medium. We find that switching the magnetic field in the present configuration results in widening the gap between the two bulk bands and a Zeeman-like splitting of the surface-polariton modes at higher wave vectors. While in the zero magnetic field there are no bulk or surface modes below ω_{pB}, in a nonzero magnetic field it is ω_c below which there are no bona fide bulk or surface excitations. In the pseudosurface wave region (below ω_c), we find only an ill-behaved bulk band whose both edges decrease in frequency with the increasing wave vector. Finally, it is worth commenting that while doing the numerical computation for a transcendental function (like our dispersion relations) one *should* always write the trigonometric functions in terms of exponentials with *negative* exponents in order to avoid the risk of getting absurd (or unphysical) results.

Note Added in Proof. We have succeeded in doing an analytical diagnosis of the dispersion relation for surface magnetoplasmons in the nonretardation limit. Therefore, we can understand the asymptotic limit approached by the lowest SP mode in the $\mathbf{B}_0 \neq 0$ case. The analytical results will be incorporated in a planned, forthcoming publication on metallic superlattices in a strong magnetic field.

ACKNOWLEDGMENTS

The author would like to thank Professor P. Halevi for stimulating discussions and Professor R. F. Wallis for useful communication.

[1]For a recent review, see L. Esaki, in *Synthetic Modulated Structures*, edited by L. Chang and B. C. Giessen (Academic, New York, 1985).

[2]M. S. Kushwaha and P. Halevi, Phys. Rev. B **38**, 12428 (1988); **36**, 5960 (1987); **35**, 3879 (1987).

[3]M. S. Kushwaha, Phys. Rev. B **35**, 3871 (1987); **37**, 1019 (1988).

[4]M. S. Kushwaha, Phys. Rev. B **33**, 1257 (1986); Solid State Electron. **29**, 31 (1986).

[5]T. Ando, Surf. Sci. **73**, 1 (1978); T. Ando, A. B. Fowler, and F. Stern, Rev. Mod. Phys. **54**, 437 (1982).

[6]A. L. Fetter, Ann. Phys. (N.Y.) **88**, 1 (1974); D. Grecu, Phys. Rev. B **8**, 1958 (1973); S. Das Sarma and J. J. Quinn, *ibid.* **25**, 7603 (1982); **27**, 6516 (1983), and references therein.

[7]G. F. Giuliani and J. J. Quinn, Phys. Rev. Lett. **51**, 919 (1983).

[8]A. C. Tselis and J. J. Quinn, Phys. Rev. B **29**, 3318 (1984).

[9]R. E. Camley and D. L. Mills, Phys. Rev. B **29**, 1695 (1984); B. L. Johnson, J. T. Weiler, and R. E. Camley, *ibid.* **32**, 6544 (1985).

[10]J. K. Jain and P. B. Allen, Phys. Rev. B **32**, 997 (1985).

[11]R. Szenics, R. F. Wallis, G. F. Giuliani, and J. J. Quinn, Surf. Sci. **166**, 45 (1986).

[12]M. S. Kushwaha, J. Appl. Phys. **62**, 1895 (1987); **63**, 5612 (1988); **65**, 3303(E) (1989).

[13]R. F. Wallis, R. Szenics, J. J. Quinn, and G. F. Giuliani, Phys. Rev. B **36**, 1218 (1987); R. F. Wallis and J. J. Quinn, *ibid.* **38**, 4205 (1988).

[14]J. K. Jain and S. Das Sarma, Phys. Rev. B **36**, 5949 (1987).

[15]M. S. Kushwaha, J. Phys. Chem. Solids **49**, 165 (1988).

[16]R. F. Wallis, in *Electromagnetic Surface Modes,* edited by A. D. Boardman (Wiley, New York, 1982).